INC-MPPT Algorithm for Maximizing Energy Conversion Efficiency of Thermoelectric Generating System

M.Elzalik[a], Hegazy Rezk[c,d] , E.G.Shehata[c] ,Jean Thomas[b] and R.Mostafa[a]

[a] Process Control Technology Dept., Faculty of Industrial Education, Beni-Suef University, Egypt
[b] Electrical Engineering Department, Faculty of Engineering, Beni-Suef University, Egypt
[c] Electrical Engineering Department, Faculty of Engineering, Minia University, Egypt
[d] College of Engineering at Wadi Addawaser, Prince Sattam Bin Abdulaziz University, KSA
mohamed.abdelbar@techedu.bsu.edu.eg

ABSTRACT

Thermoelectric Generator (TEG) is one of the renewable energy sources that can generate electrical power from waste heat energy from geothermal, solar or industrial plants. To maximizing the output power of a TEG system, the internal resistance of the TEG module must be matched with the load resistance. In this paper, TEG system has been simulated and implemented with a DC-to-DC boost converter including the maximum power point tracker (MPPT) control algorithms to maximize the energy conversion efficiency. Incremental Conductance (INC-MPPT) has been simulated with the MATLAB-Simulink and implemented with Arduino microcontroller and tested at different operating conditions. Simulation and experimental results showed that the experimental TEG system and simulation model have maximized the electrical output power of the TEG module with good accuracy and faster response to track the MPP at rapid changes of temperature on both sides of the module. The experimental results show that the harvested power duplicated by more than six times using the INC-MPPT algorithm applied in comparing with the connection without MPPT at the same operating condition.

KEYWORDS

Thermoelectric Generators; DC-DC boost converter; waste heat recovery; Incremental Conductance; MPPT; Energy Efficiency.

1- INTRODUCTION

Thermoelectric Generator (TEG) is one of the renewable energy sources that can minimize the release of the CO_2 and other harmful gases produced in case of fossil fuel. The heat energy from different renewable energy sources such as geothermal, solar [1], [2], or waste heat from any operational processes such as power plants can be converted into DC electrical power using Thermoelectric Generating (TEG) technology depending on the Seebeck effect.

To date, TEG Technology is commonly used to recover the waste heat energy from power plants, which increases their efficiency. Also, there are many other applications for thermoelectric generators such as medical, automotive, sensors, stove and space exploration applications [3]–[9]. Thermoelectric generator module is based on semiconductors and consists of a thermocouple made of p and n-type semiconductors pellets; these pellets are connected electrically in series together to increase the output voltage and placed between two ceramic wafers to form a TEG module. TEG module are placed between two heat exchangers. One forms the hot side and the other forms the cold side. The electrical output power of the module depend on the temperature difference between the hot and cold sides of the TEG module which is proportional to the heat energy flows from the hot side to the cold side of the heat exchangers[10].

In recent years, many studies have been presented to improve the efficiency of the TEG modules by improving the semiconductor materials[3], [11]–[14], heat exchanger of the hot and cold sides to decrease the thermal resistance[15]–[18], and improving the electronic interface circuit with the external load to maximize the output power[19]–[22].

TEG module operated at the maximum output power when the electrical resistance of the external load is matched with the internal resistance of the module[9]. In most practical applications, the different temperature applied on both sides of the TEG module is not constant and the value of the electrical resistance of the external load is not matched with the internal resistance when it is directly connected with the TEG module, as a result of this, the electrical output voltage of the module is affected directly by these changes and doesn't work or extract the maximum output power of the TEG module. So, the external load must be connected with the TEG module via a DC-DC converter with a MPPT control algorithm to adjust the load resistance with the internal resistance and maximize the harvested output power at any variation in temperature at different operating conditions.

Up to date, there are several techniques that have been reported for MPPT in photovoltaic (PV)systems[23], [24], and most of these techniques can be used in TEG system , each algorithm has its own lineaments and is distinguished in many aspects like type and number of sensors required, intricacy, cost, range of tracking efficiency, kind of hardware required for implementing the algorithm, accuracy, speed convergence and application. Incremental Conductance (INC), the most popular technique, is applied to maximizing the output power in the PV systems, because this

method provides major advantages over other techniques like speed and accuracy. It is very good and adjustable and has less fluctuation around MPP[23], [25].

In this paper, TEG test bench including the design of the heat exchanger of the hot and cold sides has been proposed to simulate the different operating condition of the waste heat energy sources. TEG system including a TEG module and a DC- to DC boost converter integrated with incremental conductance (INC-MPPT) has been analyzed and simulated with MATLAB-Simulink and implemented with the Arduino microcontroller. Arduino is used to control in the duty cycle of the DC boost converter to maximize the harvested output power from the TEG. Also, it used as a data acquisition system to measure the electrical current, voltage and temperature on both sides of the TEG module and send it to the personal computer. Finally, the electrical performance of the TEG system has been analyzed and compared with and without applying INC-MPPT algorithm.

2- MODELING OF THERMOELECTRIC GENERATOR

Up to date, semiconductors are the basic materials used to fabricate the thermoelectric generator modules. TEG consists of a thermocouple made of p and n-type semiconductors pellets that are connected in series to increase the output voltage of the TEG module. These pellets are arranged between two ceramic wafers to form the hot and cold sides of the TEG module as illustrated in Fig.1.

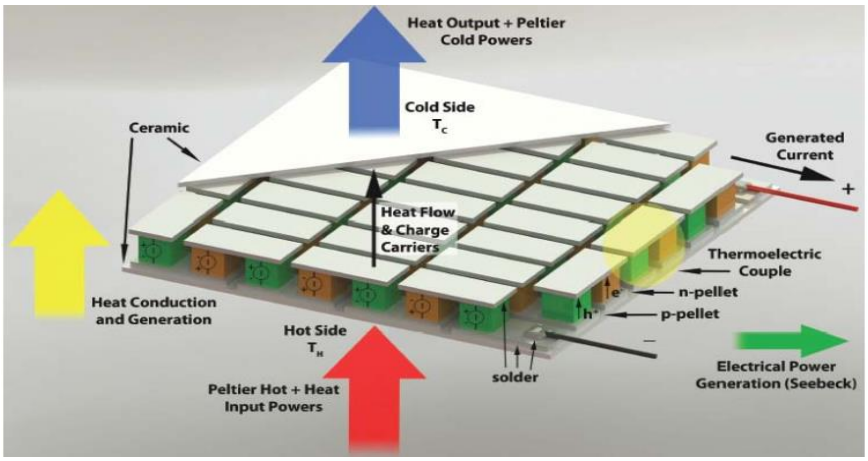

Fig.1 Schematic Diagram of a thermoelectric generator showing the main physical effects[26].

Thermoelectric technology is based on Seebeck Effect, Peltier Effect, Thomson Effect and Joule heating effect to convert the heat energy to electrical power and vice versa. When the temperature difference is applied on both sides of the TEG modules the electrical open circuit voltage (V_{oc}) will be generated on the terminals. This voltage mainly depends on the Seebeck coefficient (α) and the value of the temperature difference (ΔT). open circuit voltage can be calculated by the following relation[27], [28]:

$$V_{oc} = \alpha \times \Delta T \quad (1)$$

According to the first law of thermodynamic, at heat energy balance, the heat energy flows through a junction from high value temperature to low value temperature ($Q_h \longrightarrow Q_c$) as given by the following[28], [29]:

$$Q_h = \alpha I_{teg} T_h + K\Delta T - \frac{1}{2} {I_{teg}}^2 R_{int} \quad (2)$$

$$Q_c = \alpha I_{teg} T_c + K\Delta T + \frac{1}{2} {I_{teg}}^2 R_{int} \quad (3)$$

where Q_h denotes the heat current at hot temperature, Q_c is the heat current at cold temperature and K is the thermal conductance, R_{int} is the total pellets internal resistance, ΔT is the temperature difference between the hot and cold side ($\Delta T = T_h - T_c$), α is Seebeck coefficient

The output power of the TEG module is equal to the difference between Q_h and Q_c and is given by the following equation:

$$P_{teg} = Q_h - Q_c = \alpha \Delta T I_{teg} - I_{teg}^2 R_{int} \quad = \left(\alpha \Delta T - I_{teg} R_{int}\right) I_{teg}$$
$$= V_{teg} I_{teg} \quad (4)$$

Where V_{teg} is the electrical voltage on the load resistor R_L.,

TEG module can be represented by electrical equivalent circuit that consists of voltage source (V_{oc})connected in series with electrical resistance (R_{int}) and connected with the electrical load as illustrated in Fig.2.

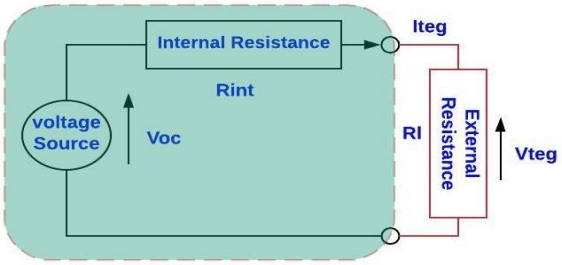

Fig.2 equivalent circuit of the TEG module

From the TEG module equivalent circuit, the total value of the electrical voltage across the load (V_{teg}) can be concluded by Ohm's Law and the open circuit voltage by the following equation.

$$V_{teg} = \alpha \Delta T - I_{teg} R_{int} \quad = V_{oc} - I_{teg} R_{int} \quad = I_{teg} R_L \quad (5)$$

The maximum power of the TEG module is achieved when the internal resistance equals the value of the external load resistance ($R_{int} = R_L$), the voltage (V_{mpp}), current (I_{mpp}) and power (P_{mpp}) at the maximum power point (MPP) are given by the following equations.

$$V_{mpp} = \frac{\alpha \Delta T}{2} = \frac{1}{2} V_{oc} \quad (6)$$

$$I_{mpp} = \frac{\alpha \Delta T}{2R_{int}} = \frac{V_{oc}}{2R_{int}} \quad (7)$$

$$P_{mpp} = V_{mpp} I_{mpp} = \frac{\alpha^2 \Delta T^2}{4R_{int}} = \frac{V_{oc}^2}{4R_{int}} \quad (8)$$

The electrical characteristics specifications of the commercial TEG modules HZ-14HV shown in table. 1.[30], have been used for the simulation model with MATLAB-Simulink. The same TEG module (HZ-14HV) has been used in the experimental test for this study.

Table.1 Specifications of the TEG HZ-14HV module.

Characteristics	Specification
Temperature of the Hot side	250 ℃
Temperature of the cold side	50 ℃
Open circuit voltage	7.91 V
Short circuit current	7.979 A
Matched load resistance	0.991Ω
Voltage at matched load	3.95 V
Current at matched load	3.9895 A
Power at matched load	15.7747 W

3- DC-DC BOOST CONVERTER AND MPPT

The maximizing output power circuit of the proposed TEG system is consisting of a DC-DC converter integrated with INC-MPPT control algorithm as shown in Fig.3. The main function of the INC-MPPT algorithm is to move the electrical operating point of a circuit by receiving the amount of the output voltage or/and electrical current of TEG and update the value of the duty cycle of the DC-DC boost converter to correspond the electrical load characteristics, so that the TEG operates at a voltage and current which leads to the transfer the maximum power to the load.

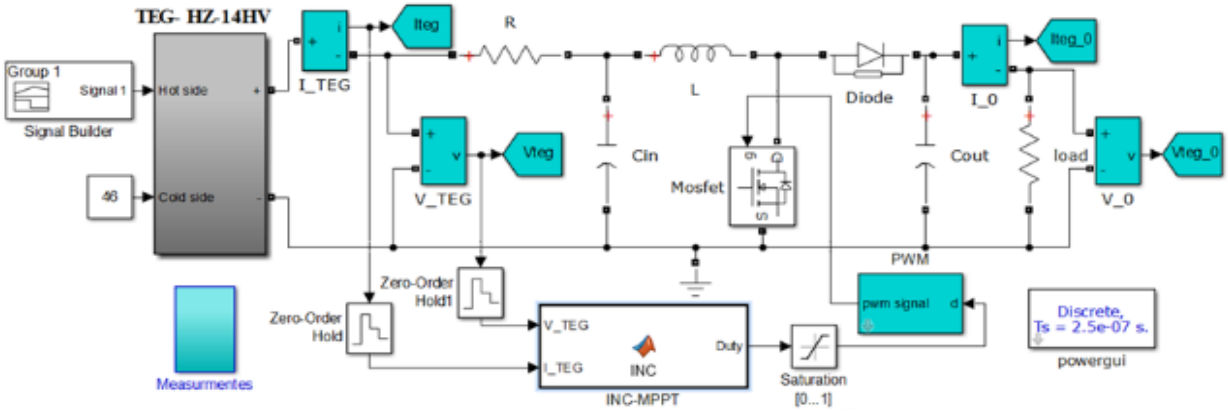

Fig.3 MATLAB/Simulink models of INC-MPPT and HZ-14HV TEG module

The DC-DC boost converter is designed by applying the following equations to select the optimal values of the inductor and the capacitors to operate in the continues mode[31]. The converter duty cycle is the most important key for selecting boost converter components and controlling of the DC-DC converter to maximize the output power from the TEG system, and it can be given from the following relation:

$$D = 1 - \frac{V_{in(\min)} \times \eta_{conv}}{V_{out}} \quad and \quad 0 \le D \le 1 \tag{9}$$

Where $V_{in(\min)}$ is the minimum value of the input voltage that can be supplied to the converter, η_{conv} is the efficiency of the converter and V_{out} is the required output voltage and given by:

$$V_{out} = \frac{1}{1-D} \times V_{in} \tag{10}$$

The inductor value must be greater than the minimum inductor (L_{min}) as given by:

$$L_{min} \ge \frac{V_{in} \times (V_{out} - V_{in})}{\Delta I_L \times F_{SW} \times V_{out}} \tag{11}$$

Where F_{SW} is the switching frequency applied on the MOSFET and ΔI_L is the ripple current for the inductor, it can be estimated from 20% to 40% from the maximum output current $I_{out(\max)}$ and given by.

$$\Delta I_L = 0 \cdot 2 \times I_{out(max)} \times \frac{V_{in}}{V_{out}} \tag{12}$$

$$or$$

$$\Delta I_L = \frac{V_{in(min)} \times D}{F_{SW} \times L} \tag{13}$$

Maximum output current of the power electronic switches (MOSFET $I_{SW(\max)}$ and Diode $I_{D(\max)}$) can be estimated from the following equations respectively:

$$I_{SW(\max)} = \left[\frac{\Delta I_L}{2} + \frac{I_{out(\max)}}{(1-D)}\right] \tag{14}$$

$$I_{D(\max)} = I_{out(\max)} \tag{15}$$

The minimum value of the input capacitor can be selected depending on the stability requirement on the input voltage for the peak current requirement of a boost converter. Also, the output capacitor value must be greater than the minimum value $C_{out(\min)}$ to reduce the ripple of the output voltage as given by:

$$C_{out(\min)} \ge \frac{I_{out(\max)} \times D}{\Delta V_{out} \times F_{SW}} \tag{16}$$

DC-DC boost converter has been simulated and implemented with 80NF70 power MOSFET, TLP250 MOSFET Driver, STPS2045 diode, 0.5mH inductor, 20KHz

switching frequency, 16Ω load resistance, $1000\mu F$, $1800\mu F$ input and output capacitors.

INC-MPPT control algorithm is depends on the fact that the power derivative with respect to its voltage is zero at the MPP as written in eq.19 and the basic rules of INC-MPPT have been written as in eq.18.

$$\frac{\mathrm{d}P_{TEG}}{\mathrm{d}V_{TEG}} = 0 \Longrightarrow \frac{\mathrm{d}(V_{TEG}I_{TEG})}{\mathrm{d}V_{TEG}} = I_{TEG} + V_{TEG}\frac{dI_{TEG}}{dV_{TEG}} = 0 \tag{17}$$

$$\begin{cases} \dfrac{\Delta I_{TEG}}{\Delta V_{TEG}} = -\dfrac{I_{TEG}}{V_{TEG}} & at\ MPP\ ; \\ \dfrac{\Delta I_{TEG}}{\Delta V_{TEG}} > -\dfrac{I_{TEG}}{V_{TEG}} & at\ left\ of\ MPP\ ; \\ \dfrac{\Delta I_{TEG}}{\Delta V_{TEG}} < -\dfrac{I_{TEG}}{V_{TEG}} & at\ Right\ of\ MPP; \end{cases} \tag{18}$$

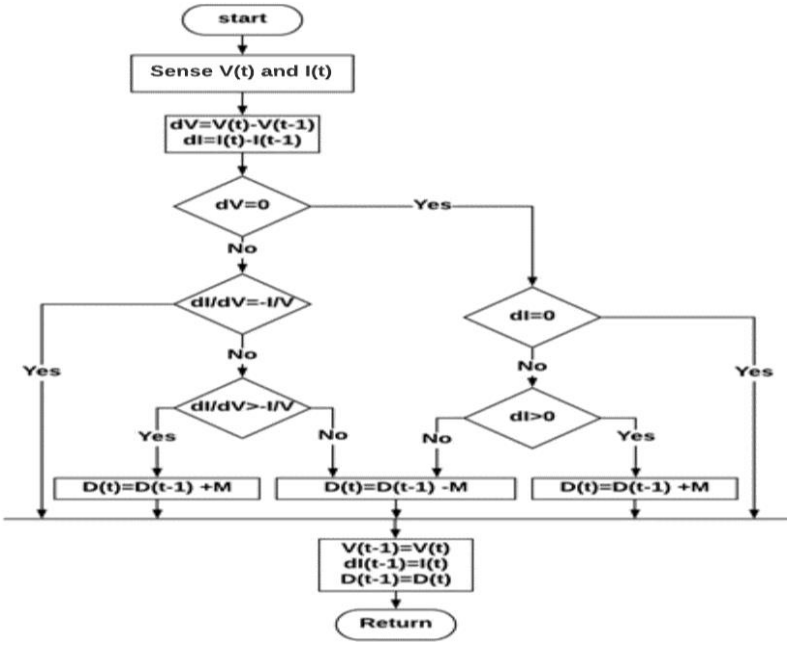

Fig. 4 Flowchart of INC- MPPT control algorithm.

The flowchart of INC-MPPT control algorithm is shown in Fig.4, which used in the simulation model and implemented on the Arduino microcontroller. The control algorithm is started by measuring the output currant and voltage of TEG module and according to the rules (in eq.18 and in Fig.4) the duty cycle (D) has been increased or decreased by step value (M) to estimate directly the optimal value of (D) which obtain and transfers the maximum power of the TEG module to the load.

4- EXPERIMENTAL SETUP

The Proposed Thermoelectric Generator test bench has been designed to test the Thermoelectric Generator module at different operating conditions, several components are involved in this system:

- A hot side heat exchanger to maximizing the heat transferring from the heat energy source to the hot side of the TEG module.
- A cold side heat exchanger to liberate the heat from the cold side of the TEG module and increase the temperature difference between the both sides of the TEG .
- Mechanical frame to integrate and fixe the TEG module with the heat exchangers.
- mechanical springs are used to distribute the mechanical pressure regularly on the TEG module surface.
- Chiller and water pump, chiller is used to cool water and water pump is used to cycle the colded water through the cold side exchanger.
- Electrical heater with temperature controller to adjust the hot side temperature
- DC-to-DC boost converter connected in series with TEG module and resistive load.
- Current, voltage, temperature sensors and Arduino microcontroller to control and monitor the TEG voltage, current, power and different values of temperature on the hot and cold sides.

The block diagram of the proposed TEG testing system is shown in Fig.5 and the hardware experimental set up is shown in Fig.6.

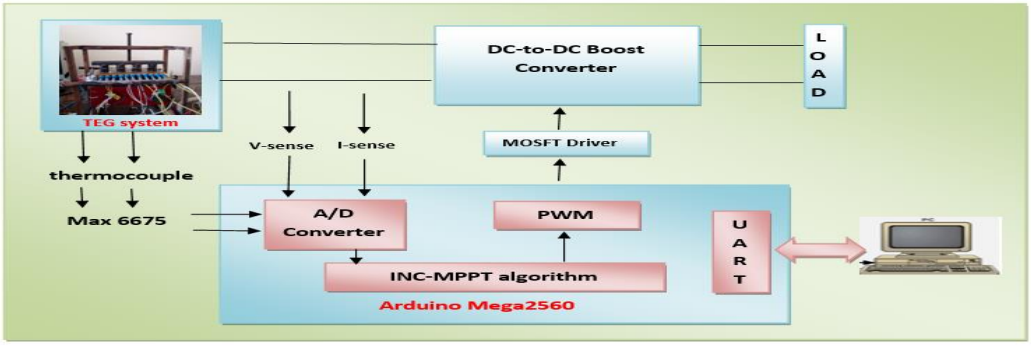

Fig. 5 The block diagram of the proposed TEG testing system.

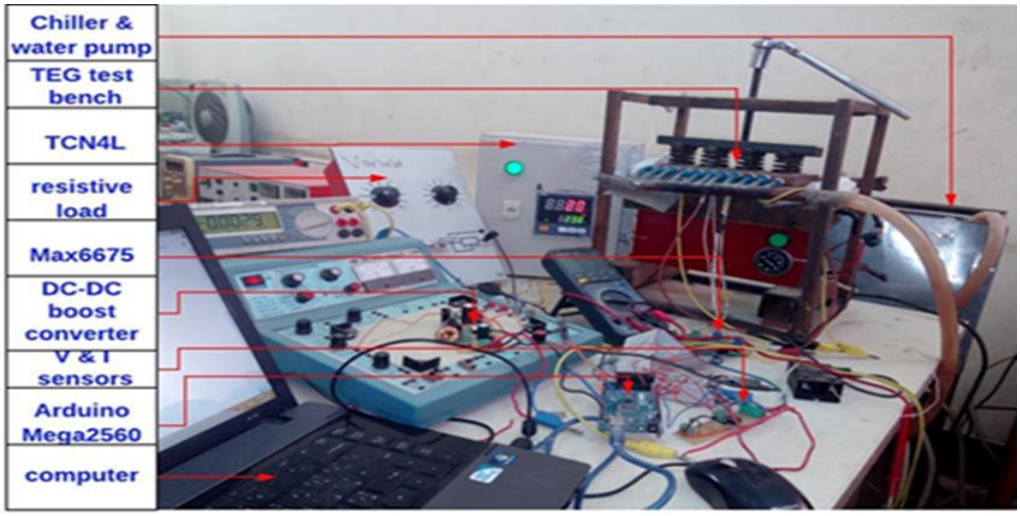

Fig. 6 hardware experimental set up proposed TEG testing system.

TEG module has been placed between the two heat exchangers of the hot and cold side with the applied mechanical pressure and tested at different operating conditions. Also, it is connected to the DC-DC converter integrated with the INC-MPPT control algorithm. TEG system has been tested when the hot and cold side temperature are increased together and tested at rapidly change in the temperature difference of the hot and cold side of the TEG module to analyze and examine the electrical performance of the proposed TEG system with INC-MPPT at different operating conditions. At all tested cases, the current, voltage and temperature on the hot and cold side have been measured every $500ms$ and stored on the computer using Arduino microcontrollers. The experimental results of the different testes will be discussed in the following section.

5- RESULTS AND DISCUSSION

The proposed TEG system has been simulated using MATLAB-Simulink including HZ-14HV TEG module and DC-DC boost converter with INC-MPPT algorithm as shown in Fig.3 and it has been tested at 46℃ cold side temperature and different values of hot side temperature to examine the electrical performance of the INC-MPPT control algorithm at rapidly changed in the temperature difference on the TEG module which was being changed every $0.1ms$ at 125℃ to 221 ℃ at final simulation time $0.5ms$ as shown in Fig.7

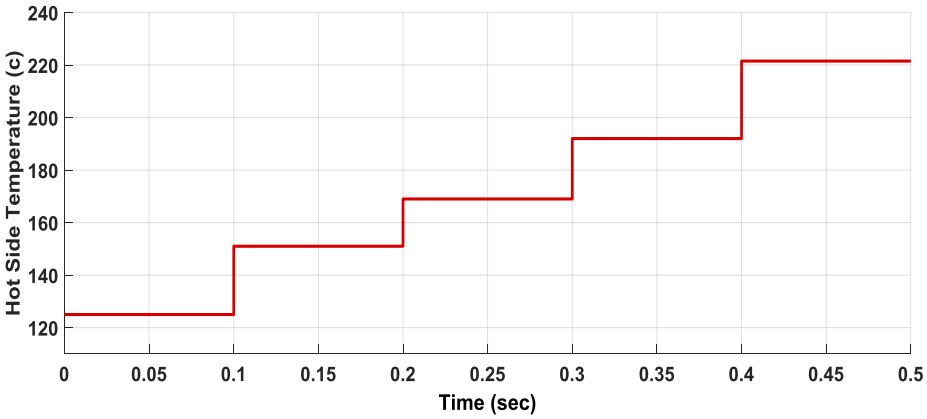

Fig.7 different values of the hot temperature (125; 151;169; 192; 221℃) applied on the simulation test.

DC-DC boost converter has been simulated including the real parameters of the power electronics switches (MOSFT and diode), inductor and capacitors. Simulation results of the input and output power, voltage and current of the boost converter with INC-MPPT at different values of the hot side temperature are shown in Fig.8. The changing in the converter duty cycle to track the maximum output power during varying the applied temperature on the hot side is shown in Fig.9. The heat energy of the hot side Q_h and cold side Q_c (from eq.2 and eq.3 respectively), the efficiency of the TEG module and the efficiency of the DC-DC boost converter have been estimated and shown in Fig.10.

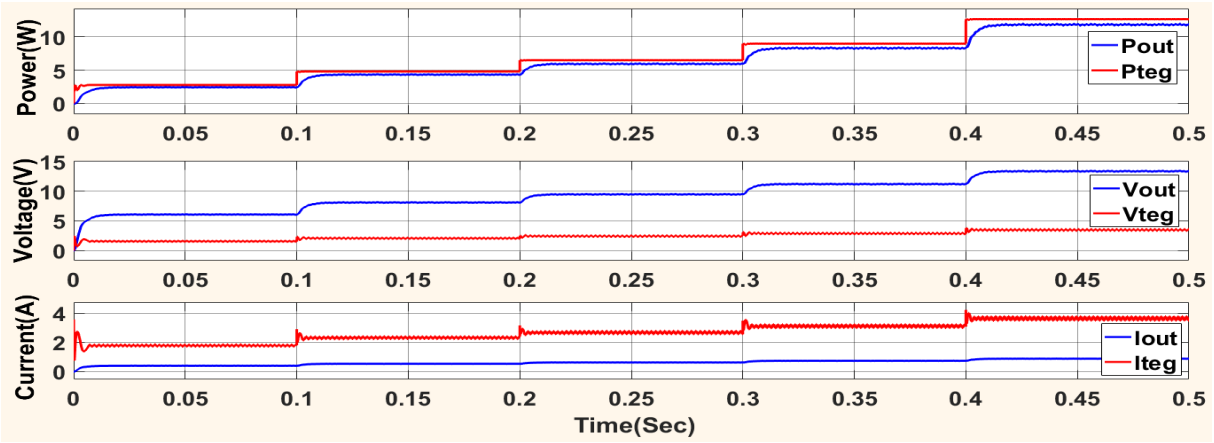

Fig.8 Simulation results of the input and output power, voltage and current of the boost converter with INC-MPPT and different values of a hot side temperature.

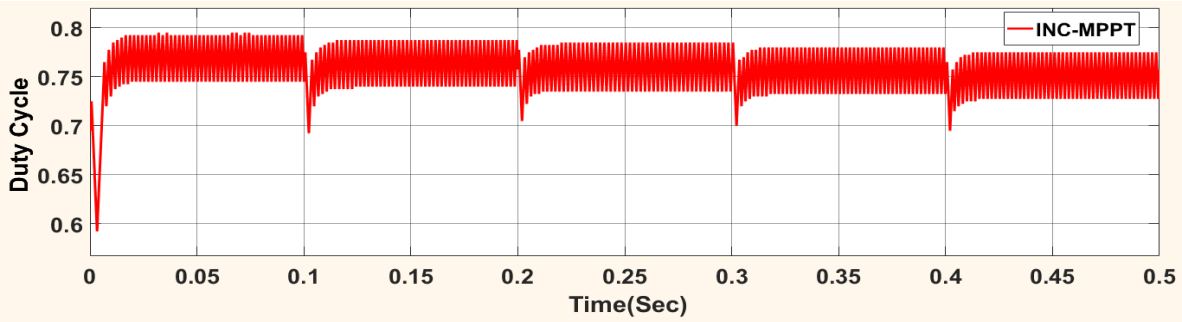

Fig.9 The change in the duty cycle at the different values of a hot side temperature.

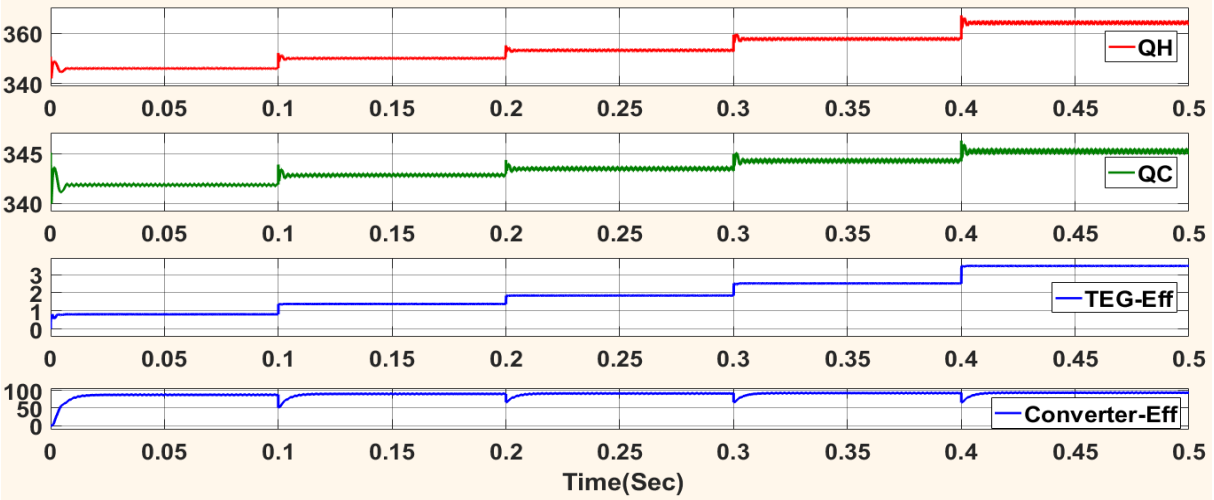

Fig.10 Simulation results of the heat energy, TEG module and converter efficiency at INC-MPPT and different values of the hot side temperature.

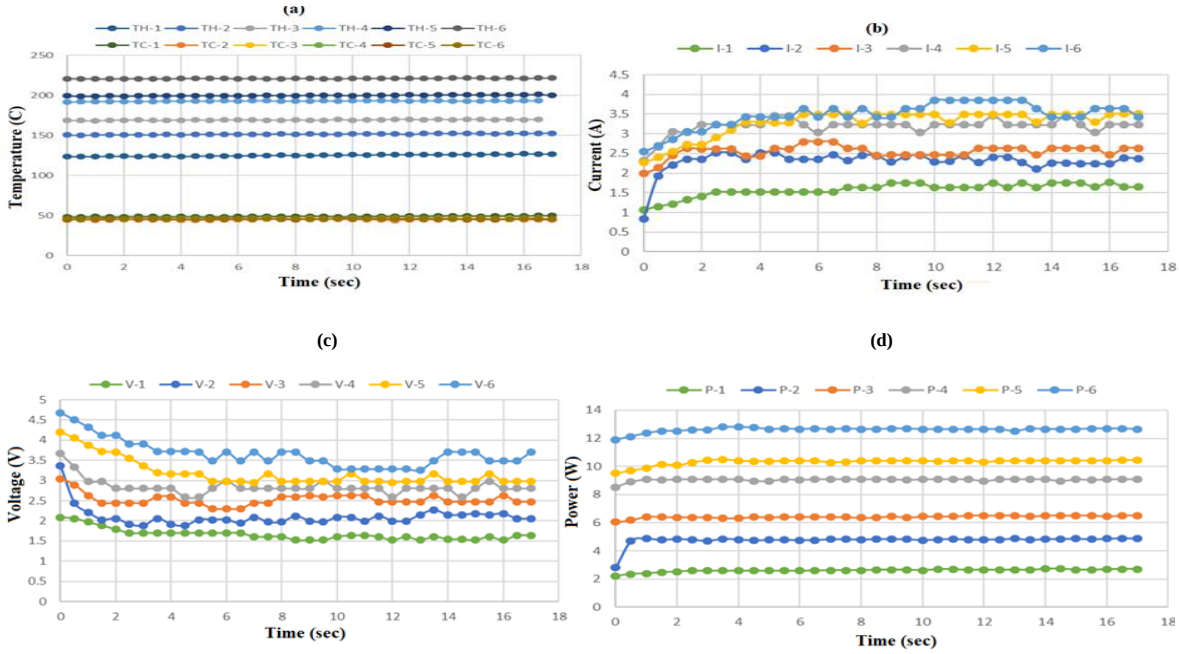

Fig.11 Experimental measurements of INC-MPPT at constant temperature and different values of temperature applied on the hot side, (a) hot and cold sides temperature, (b) current, (c) voltage and (d) power of the INC-MPPT.

The experimental tests have been started by adjusting the hot and cold side of the TEG module, as the Arduino microcontroller was measuring the current, voltage and hot and cold side temperature every $500ms$ and saving them on the computer. TEG module has been tested at different operating conditions. First test, when the cold side was set at $46℃$ and the hot side was set at $125;\ 151\cdot5;169;\ 192;\ 200;\ 221\ ℃$ as shown in Fig.11(a). In this test, the TEG module has been tested at constant temperature to investigate the INC-MPPT control algorithm when its applied to recover the low waste heat energy in ranged between $120\ to\ 220\ ℃$. The output current, voltage and power of the TEG module when the INC-MPPT algorithm is applied to maximize the output power are shown in Fig.11(b, c & d) through $17sec$ timing test. The experimental results show that the proposed TEG system including the INC-MPPT control algorithm can achieve the maximum output power through $1.5\ sec$ with less fluctuation around the MPP as shown in Fig.11(d).

TEG system has been tested and compared when the TEG module was connected to 16Ω resistive load through a DC-DC boost converter integrated with INC-MPPT control algorithm and directly connect without INC-MPPT at $205.4℃$ hot side temperature and $46.9℃$ cold side temperature as shown in Fig.12. This figure includes the current, the voltage and the power with appling INC-MPPT through the time from $0\ to\ 25sec$ and direct connect without INC-MPPT at the time from $26\ to\ 29sec$. The experimental results show that the output power using the INC-MPPT algorithm applied is $11.9W$ and $1.9W$ without using INC-MPPT at the same resistive load (16Ω), the same applied temperature and the same operating conditions. This mean that the harvested power has duplicated by 6.26 time by using MPPT.

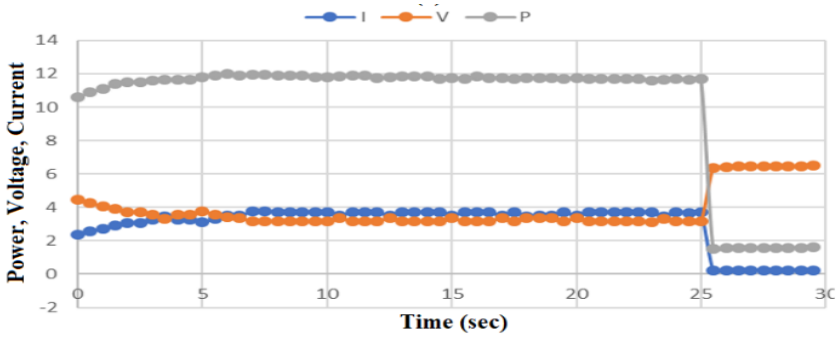

Fig.12 Experimental results of the current, voltage and power at TH = 205.4℃ and TC = 46.9℃ with INC-MPPT and direct connect without MPPT (hot side and cold side are constant).

Also, TEG system with the INC-MPPT has been tested when hot side temperature was being increased through $192sec$, and cold side temperature was being decreased as shown in Fig.13(a). The experimental results of the current, voltage and power at these changes of the hot and cold side temperature are shown in Fig.13(b).

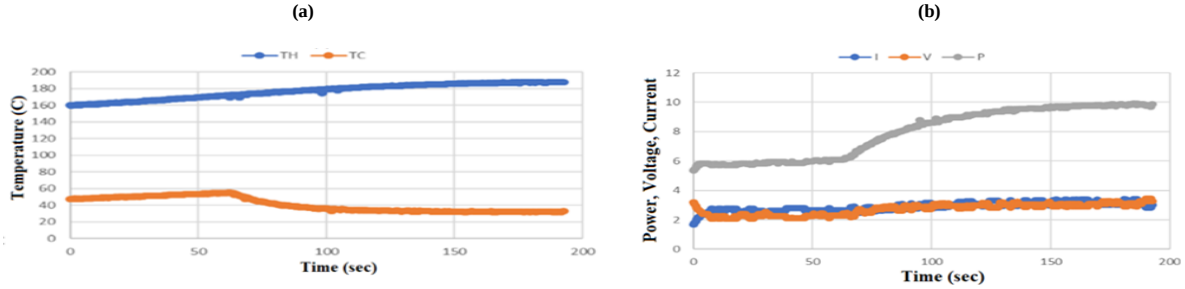

Fig.13 Experimental measurements of INC-MPPT when hot side is increased, and cold side is decreased, (a)hot and cold sides temperature, (b) current, voltage and power at this temperature.

In the final test, the electrical performance of the INC-MPPT has been tested when the hot side and cold side temperature of the TEG module are increased as shown in Fig.14(a), the effect of these changes on the output current, voltage and power are shown in Fig.14(b).

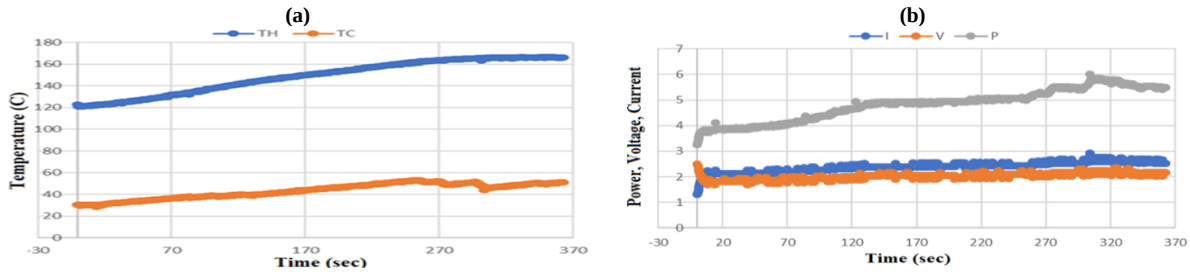

Fig.14 Experimental measurements of INC-MPPT when the hot side and cold side temperature are increased and rapidly changed, (a)hot and cold sides temperature, (b) current, voltage and power at this temperature.

Experimental results in Fig.13(b) and Fig.14(b) show that the output power directly depends on the value of the different temperature between the hot and cold side temperature, in Fig.13(a), the hot side temperature has been increased from $160.25℃\ to\ 187.7℃$ in the time test $(192sec)$ and the cold side temperature values have been increased from $47.5℃\ to\ 55℃$ though time from $0\ to\ 62.2sec$ which keep the temperature difference between the hot and cold side around $120℃$ at the time from $0\ to\ 62.2sec$, so the output power, voltage and current are extremely constant at this time as shown in Fig.13(b), but through the time $63\ to\ 192\ sec$ the cold side temperature values are decreased from $54.75℃\ to\ 32.75℃$ and hot side temperature values are increased as in Fig.13(a), which make the output power, voltage and current increase at this time as shown in Fig.13(b). Also, the changes of the hot and cold side temperature as shown in Fig.14(a), directly affects the output power, voltage and current as shown in Fig.14(b).

Experimental and simulation results are compared with the manufacturing data sheet at different values of temperature as shown in Fig.15(a and b). Experimental and simulation results show that the efficiency of the INC-MPPT control algorithm, which estimated from eq.19, has been changed from $96.9\%\ to\ 98.6\%$ for the simulation tests and from $88\%\ to\ 98\ \%$ for the experimental testes depending on the temperature differences applied on the TEG module.

$$\text{Efficiency } \% = \frac{output\ power\ of\ MPPT\ algorithm}{power\ of\ manufacturing\ data\ sheet} \times 100 \qquad (19)$$

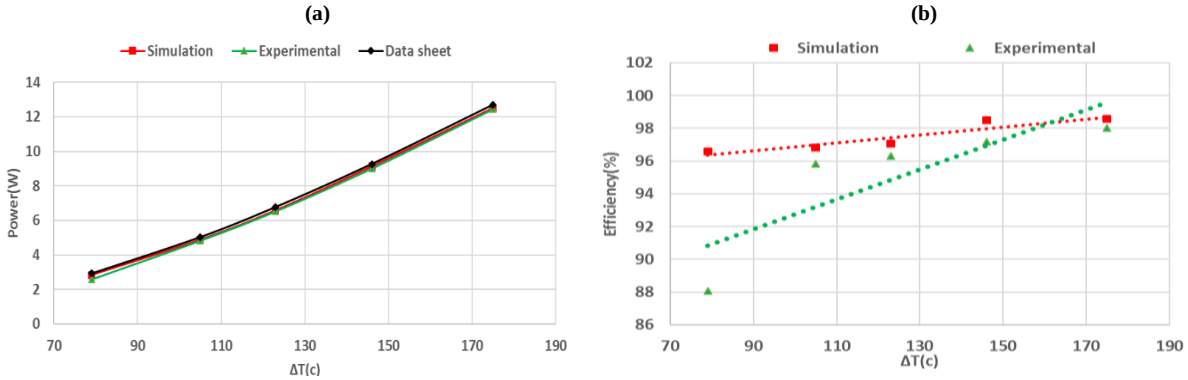

Fig.15 Experimental and simulation results comparing with the manufacturing data sheet at the different values of the temperature differences (a) Average power of the TEG module, (b) INC-MPPT efficiency

6- CONCLUSION.

In this paper, TEG testing system has been proposed and implemented to simulate different operating conditions of waste heat energy applications. Commercial HZ-14HV TEG module that connected to the DC-DC boost converter with INC-MPPT control algorithm has been simulated with the MATLAB/Simulink, implemented and tested at different operating conditions. Low cost Arduino microcontroller has been used to control the DC-DC boost converter and maximize the output power of the TEG module and used as a data acquisition system to measure current, voltage and hot and

cold side temperature and store them on the computer. Simulation and experimental results prove that the proposed TEG testing system with the INC-MPPT control algorithm can extract the maximum output power of the TEG module with good accuracy and faster response to track the MPP at the rapidly changing in temperature and at any operating conditions.

7- REFERENCES.

[1] P. Sundarraj, S. S. Roy, R. A. Taylor, and D. Maity, "Performance analysis of a hybrid solar thermoelectric generator," *Energy Sources, Part A Recover. Util. Environ. Eff.*, vol. 38, no. 20, pp. 2977–2984, 2016.

[2] S. Shanmugam, A. R. Veerappan, and M. Eswaramoorthy, "An experimental evaluation of energy and exergy efficiency of a solar parabolic dish thermoelectric power generator," *Energy Sources, Part A Recover. Util. Environ. Eff.*, vol. 36, no. 17, pp. 1865–1870, 2014.

[3] A. R. M. Siddique, S. Mahmud, and B. Van Heyst, "A review of the state of the science on wearable thermoelectric power generators (TEGs) and their existing challenges," *Renew. Sustain. Energy Rev.*, vol. 73, no. December 2016, pp. 730–744, 2017.

[4] U. P. T. O. Now and G. Description, "Experimental 5-Kw Thermoelectric Generator," *Energy*, vol. 2, pp. 275–279, 1962.

[5] W. He, G. Zhang, X. Zhang, J. Ji, G. Li, and X. Zhao, "Recent development and application of thermoelectric generator and cooler," *Appl. Energy*, vol. 143, pp. 1–25, 2015.

[6] C. Yu and K. T. Chau, "Thermoelectric automotive waste heat energy recovery using maximum power point tracking," *Energy Convers. Manag.*, vol. 50, no. 6, pp. 1506–1512, 2009.

[7] S. Cristina and A. Vale, "Thermoelectric generator from space to automotive sector- model and design for commercial and heavy duty vehicles," no. November, 2015.

[8] K. Nithyanandam and R. L. Mahajan, "Evaluation of metal foam based thermoelectric generators for automobile waste heat recovery," *Int. J. Heat Mass Transf.*, vol. 122, pp. 877–883, 2018.

[9] H. B. Gao, G. H. Huang, H. J. Li, Z. G. Qu, and Y. J. Zhang, "Development of stove-powered thermoelectric generators: A review," *Appl. Therm. Eng.*, vol. 96, pp. 297–310, 2016.

[10] P. Aranguren, D. Astrain, and A. Martínez, "Study of complete thermoelectric generator behavior including water-to-ambient heat dissipation on the cold side," *J. Electron. Mater.*, vol. 43, no. 6, pp. 2320–2330, 2014.

[11] D. Champier, "Thermoelectric generators: A review of applications," *Energy Convers. Manag.*, vol. 140, pp. 167–181, 2017.

[12] Y. Yin, B. Tudu, and A. Tiwari, "Recent advances in oxide thermoelectric materials and modules," *Vaccum*, vol. 146, pp. 356–374, 2017.

[13] S. Twaha, J. Zhu, Y. Yan, and B. Li, "A comprehensive review of thermoelectric technology : Materials , applications , modelling and performance improvement," vol. 65, pp. 698–726, 2016.

[14] R. Zybała, M. Schmidt, K. Kaszyca, Ł. Ciupiński, M. J. Kruszewski, and K. Pietrzak, "Method and Apparatus for Determining Operational Parameters of Thermoelectric Modules," *J. Electron. Mater.*, vol. 45, no. 10, pp. 5223–5231, 2016.

[15] S. C. Tzeng, T. M. Jeng, and Y. L. Lin, "Parametric study of heat-transfer design on the thermoelectric generator system," *Int. Commun. Heat Mass Transf.*, vol. 52, pp. 97–105, 2014.

[16] D. S. Patil, R. R. Arakerimath, and P. V Walke, "Thermoelectric materials and heat exchangers for power generation – A review," *Renew. Sustain. Energy Rev.*, vol. 95, no. October 2017, pp. 1–22, 2018.

[17] R. Stobart, M. A. Wijewardane, and Z. Yang, "Comprehensive analysis of thermoelectric generation systems for automotive applications," *Appl. Therm. Eng.*, vol. 112, pp. 1433–1444, 2017.

[18] S. Lv *et al.*, "Study of different heat exchange technologies influence on the performance of thermoelectric generators," *Energy Convers. Manag.*, vol. 156, no. November 2017, pp. 167–177, 2018.

[19] R. Quan, W. Zhou, G. Yang, and S. Quan, "A Hybrid Maximum Power Point Tracking Method for Automobile Exhaust Thermoelectric Generator," *J. Electron. Mater.*, vol. 46, no. 5, pp. 2676–2683, 2017.

[20] S. Manikandan and S. C. Kaushik, "Thermodynamic studies and maximum power point tracking in thermoelectric generator-thermoelectric cooler combined system," *Cryogenics (Guildf).*, vol. 67, pp. 52–62, 2015.

[21] H. Mamur and R. Ahiska, "Application of a DC-DC boost converter with maximum power point tracking for low power thermoelectric generators," *Energy Convers. Manag.*, vol. 97, pp. 265–272, 2015.

[22] Z. Qiu, K. Sun, H. Wu, J. Huang, and Y. Xing, "A high efficiency cascaded thermoelectric generation system with power balancing mechanism," *Conf. Proc. - IEEE Appl. Power Electron. Conf. Expo. - APEC*, vol. 2015–May, no. May, pp. 647–653, 2015.

[23] M. A. Danandeh and S. M. Mousavi G., "Comparative and comprehensive review of maximum power point tracking methods for PV cells," *Renew. Sustain. Energy Rev.*, vol. 82, no. July 2017, pp. 2743–2767, 2018.

[24] L. L. Jiang, R. Srivatsan, and D. L. Maskell, "Computational intelligence techniques for maximum power point tracking in PV systems: A review," *Renew. Sustain. Energy Rev.*, vol. 85, no. December 2017, pp. 14–45, 2018.

[25] T. H. Kwan and X. Wu, "The Lock-On Mechanism MPPT algorithm as applied to the hybrid photovoltaic cell and thermoelectric generator system," *Appl. Energy*, 2017.

[26] A. Montecucco and A. R. Knox, "Accurate simulation of thermoelectric power generating systems," *Appl. Energy*, vol. 118, pp. 166–172, 2014.

[27] S. Shanmugam, M. Eswaramoorthy, and A. R. Veerappan, "Modeling and analysis of a solar parabolic dish thermoelectric generator," *Energy Sources, Part A Recover. Util. Environ. Eff.*, vol. 36, no. 14, pp. 1531–1539, 2014.

[28] M. Elzalik, H. Rezk, E. G. Shehata, J. Thomas, and R. Mostafa, "Thermoelectric Power Generation System- Simulation and Experimental Investigation," *IEEE Twent. Int. Middle East Power Syst. Conf.*, vol. 978-1–5386, pp. 320–225, 2018.

[29] D. R. Karana and R. R. Sahoo, "Effect on TEG performance for waste heat recovery of automobiles using MgO and ZnO nanofluid coolants," *Case Stud. Therm. Eng.*, vol. 12, no. May, pp. 358–364, 2018.

[30] H.-Z. Technology, Inc., "Hi-Z 14W HV Thermoelectric Generator," *Hi-Z Technol. Inc.*, vol. 2, no. http://hi-com/wp-content/uploads/2017/05/Data-Sheet-HZ-14HV.pdf.

[31] B. Hauke, "Basic Calculation of a Boost Converter's Power Stage," *Texas Instruments*, no. August, pp. 1–7, 2015.